Published in final edited form as:
Biochemistry. 2012 August 21; 51(33): 6490–6492. doi:10.1021/bi300968n.

Correlation of Structure and Function in the Human Hotdog-fold Enzyme hTHEM4†

Hong Zhao[α], **Kap Lim**, **Anthony Choudry**[γ], **John A. Latham**[α], **Manish C. Pathak**[β], **Dennis Dominguez**[α], **Lusong Luo**[γ,*], **Osnat Herzberg**[β,*], and **Debra Dunaway-Mariano**[α,*]

[α]Department of Chemistry and Chemical Biology, University of New Mexico, Albuquerque, NM [β]Center for Advanced Research in Biotechnology and Institute for Bioscience and Biotechnology, University of Maryland, Rockville, Maryland [γ]Enzymology and Mechanistic Pharmacology Oncology CEDD, GlaxoSmithkline, Collegeville, PA

Abstract

Human THEM4 (hTHEM4) is comprised of a catalytically active hotdog-fold acyl-CoA thioesterase domain and an N-terminal domain of unknown fold and function. hTHEM4 has been linked to Akt1 regulation and cell apoptosis. Herein, we report the X-ray structure of hHTEM4 bound with undecan-2-one-CoA. Structure guided mutagenesis was carried out to confirm the catalytic residues. The N-terminal domain is shown to be partially comprised of irregular and flexible secondary structure, reminiscent of a protein-binding domain. We demonstrate direct hTHEM4-Akt1 binding by immunoprecipitation and by inhibition of Akt1 kinase activity, thus providing independent evidence that hTHEM4 is an Akt1 negative regulator.

The human protein hTHEM4, also known as the carboxyl-terminal modulator protein (CTMP) (1), is a two-domain protein made up of 240 amino acids (Fig. 1). Epigenetic down-regulation of hTHEM4 transcription is a common aberration in glioblastomas (2, 3). The earliest studies of hTHEM4 function showed that it interacts with membrane bound Akt1 blocking its activation by upstream protein kinases (1). Activated Akt1 is known to protect the cell from apoptosis. More recent work has painted a complex picture of the mechanism by which hTHEM4 functions to sensitize the cell to apoptosis. Firstly, an N-terminal mitochondrial location sequence (MLS) was found to direct the precursor hTHEM4 to the mitochondrial inner membrane space where it associates with the integral inner membrane protein known as the leucine zipper/EF-hand-containing trans membrane-1 protein (4). The mature hTHEM4 (MLS removed) is contained in the mitochondrial inner

†Support From NIH GM28688 (D.D-M.) and AI059733 and GM057890 (O.H.). The Advanced Photon Source is supported by the U.S. Department of Energy.
PDB accession code: 4GAH

*Address correspondence to: D.D.-M (Tel: 1-505-277-3383, dd39@unm.edu); O.H. (Tel: 240-314-6245, osnat@carb.nist.gov) or L.L (lusong.luo@beigene.com).
$Current address: BeiGene Co., Beijing, China

Supporting Information
Detailed experimental protocol, tables and figures reporting experimental results are available free of charge via the Internet at http://pubs.acs.org.

membrane space and upon induction of apoptosis it is released to the cytosol (5). Additional studies showed that phosphorylation of hTHEM4 at the mitochondrial localization signal Ser37/Ser38, blocks mitochondrial localization. In the cytoplasm, hTHEM4 reportedly associates with the heat shock protein 70 (Hsp70) thus, preventing the formation of complexes between Hsp70 and the apoptotic protease activating factor I (6).

Recently we demonstrated that the hTHEM4 is a high efficiency, broad specificity acyl-CoA thioesterase (7). The C-terminal domain (*ca*. 100 amino acids) conforms to a predicted hotdog-fold thioesterase subunit. The N-terminal domain is predicted to be ordered, however it does not have a known structural homolog. To better understand the structural basis for hTHEM4 function, it was subjected to X-ray crystallographic analysis. The MLS (residues 1-39) was removed by genetic engineering prior to co-crystallization with the inert substrate analog undecan-2-one-CoA, which is a tight binding competitive inhibitor of hTHEM4-catalyzed decanoyl-CoA hydrolysis (K_i = 0.8 ± 0.1 μM; Fig. SI1) The structure of the His_6-tagged (1) (Δ1-39)hTHEM4(undecan-2-one-CoA) complex was solved to 2.3 Å (experimental plus summary of X-ray data collection and structure refinement is provided in SI) and is shown in Fig. 1. The homodimer quaternary structure observed in the crystal structure was confirmed by native molecular mass determination of the protein in solution (*via* HPLC-SECLS-RI analysis, Table SI2).

The model of subunit A contains amino acid residues 43-81 and 106-238 whereas the residues 82-105 are structurally disordered. The subunit B model is better defined, and contains amino acid residues 43-98 and 106-244. The C-terminal hotdog-fold catalytic unit consists of two α-helices (α3), one from each subunit, oriented antiparallel to one another and packed against a continuous antiparallel β-sheet generated by the association of the two monomers (Fig. 1). In addition, residues 106-120, which are outside the hotdog-fold core, pack above the α3 helices and contribute to the dimer interface *via* a cluster of phenylalanine residues (Fig. SI2). Two undecan-2-one-CoA molecules are positioned at opposite ends of the dimer, where the substrate binding sites are formed at the subunit interface (Fig. 2). The adenine, ribose and phosphate groups of the inhibitor are perched on the protein surface at a region that defines the entrance to the active site. Ion pairs are formed between Arg206 and Lys207 and the phosphate groups and a hydrogen bond is formed between Asn183 and the C(6)NH_2 of the adenine ring, however the strength of these interactions are likely to be minimized by the polar solvent. Indeed, Ala replacement of these residues had a minimal impact on the catalytic efficiency. The k_{cat}/K_m measured for catalyzed myristoyl-CoA hydrolysis is reduced 5–fold and 3-fold, respectively for the mutants R206A and K207A but the N183A mutant is fully active (Table 1). The pantothenate unit threads through a narrow, largely hydrophobic tunnel that leads to the catalytic site (Fig. 2). CoA displays only a modest binding affinity (K_i = 81 ± 1 μM) (Fig. SI3) and the C_6-C_{12} carboxylic acid products display very weak binding affinity (K_i>1 mM) which indicates that hTHEM4 thioesterase activity is not regulated by product inhibition.

The hTHEM4 catalytic motif conforms to that of the AB clade of the hotdog-fold thioesterase family (8). Specifically, the catalytic carboxylate residue (Asp161; serves as nucleophile or base) is located on the central α-helix of one subunit whereas the thioester C=O polarizing residue (Gly153; α-helix N-terminus backbone amide NH) is located on the

opposing subunit (Fig. 2). The side chains of Thr177 and His152 also contribute to the active site. The Asp161 was replaced with Glu and with Asn to probe its role in catalysis. The hTHEM4 D161E and D161N mutants display k_{cat} values that are 42-fold and 62-fold smaller than that of the wild-type enzyme (Table 1). Asn161 can position a water nucleophile but not function in nucleophilic catalysis. Thus, the relatively small reduction in the k_{cat} of the D161N mutant is more consistent with Asp161 functioning in base catalysis than in nucleophilic catalysis. Based on its juxtaposition with the Asp161, the Thr177 is a likely partner in the positioning and activation of the water nucleophile, as has been reported for the hTHEM2 counterparts (8). The hHTEM4 T177A mutant k_{cat} value is reduced 60-fold. The His152 is located on the opposite side of the active site and is packed against the inhibitor. His152 might assist in the positioning of the substrate as suggested by the hTHEM4 H152A and H152F mutants, which showed 100-fold and 140-fold reductions in k_{cat}. Gly153, Asp161, Thr77 and H152 are conserved among eukaryote THEM4s (Fig. SI4).

The N-terminal domains of the dimer are juxtaposed in a manner that covers the α3-presenting face of the hotdog-fold (Fig. 1). Both N-terminal domains are partially disordered: 82-105 in subunit A and 99-105 in subunit B. In subunit B, residues 83-95 form an amphiphatic α-helix (α2), which caps the hydrophobic channel of the ligand binding site. The nonpolar face of α2 shields the hydrocarbon tail of the bound inhibitor. Interestingly, the hydrocarbon tail of a second inhibitor ligand is recruited to the site where it is desolvated by α3, α2 and the extended hydrocarbon tail of inhibitor 1 (Fig. 1 and Fig. SI5). Subunit A binds just one inhibitor molecule and its hydrocarbon tail assumes a curled conformation thereby minimizing contact with solvent. Notably, the region corresponding to the α2 in subunit B is disordered in subunit A. Residues 55-69 form the amphipathic helix α1, which packs against the β-sheet using its nonpolar face. Overall, the X-ray structure suggests that the N-terminal domain consists of an unusual amount of irregular secondary structure with regions of high flexibility. The tertiary structure appears to be organized along the surface of the hotdog-fold core. The observation that the removal of the N-terminal domain via genetic engineering greatly destabilizes the hotdog-fold domain (7), suggests that the two domains are not independent folding units.

Having defined the structure and catalytic activity of hTHEM4 we were positioned to explore additional functions that have been suggested by the cell biology studies (*vide supra*). Accordingly, we focused our efforts on examining hTHEM4 mediated Akt1 regulation using an *in-vitro* based approach. Firstly, hTHEM4-Akt1 binding was tested by carrying out pull-down experiments using anti-Akt1 antibody immobilized agarose beads in conjunction with the recombinant Akt1 catalytic domain and His_6-tagged hTHEM4 (details provided in SI). As shown in Fig. 3 both the His_6-hTHEM4 and hTHEM4-His_6 constructs were retained by the immobilized Akt1. The control experiment, in which Akt1 was not included, showed that hHTME4 is not retained by the beads alone. These findings demonstrate that Akt1 and hTHEM4 form a stable complex.

Finally, the potential impact of *in-vitro* hTHEM4-Akt1 complex formation on catalytic function was examined by carrying out titration experiments. For this purpose catalytically active Akt1 was prepared (9). The rate of catalyzed phosphorylation of the GSK3α peptide (10 μM) was measured at fixed Akt1 (1 nM) and ATP (50 μM) concentrations and varied

His_6-hTHEM4 (0–6 μM) concentration. The data shown in Fig. 4 were fitted to define a K_d = 0.7 ± 0.1 μM. The impact of complex formation on hTHEM4 catalytic activity was determined at fixed His_6-hTHEM4 (40 nM) and myristoyl-CoA (5 μM) concentrations and varied Akt1 concentration (0, 0.375,0.75,1.5 and 2.27 μM) in 50 mM HEPES (pH 7.5, 25 °C). The rate of catalyzed thioester hydrolysis was not inhibited but rather slightly increased (Fig. 4). Therefore, Akt1 binding does not block the hTHEM4 active site.

In conclusion, we have defined the structure and catalytic residues of hTHEM4, a two-domain protein, known to catalyze fatty acyl-CoA thioester hydrolysis (7), and to sensitize the cell to apoptosis through interaction with protein partners (1, 4–6). We have shown that hTHEM4 binding to the cell regulator Akt1 inhibits its kinase activity, which supports the data from *in-vivo* studies. Future work is focused on mapping the protein-protein binding sites on hTHEM4 and Akt1.

Supplementary Material

Refer to Web version on PubMed Central for supplementary material.

References

1. Maira SM, Galetic I, Brazil DP, Kaech S, Ingley E, Thelen M, Hemmings BA. Science. 2001; 294:374–380. [PubMed: 11598301]
2. Knobbe CB, Reifenberger J, Blaschke B, Reifenberger G. J Natl Cancer Inst. 2004; 96:483–486. [PubMed: 15026474]
3. Knobbe CB, Trampe-Kieslich A, Reifenberger G. Neuropathol Appl Neurobiol. 2005; 31:486–490. 2005. [PubMed: 16150119]
4. Piao L, Li Y, Kim SJ, Sohn KC, Yang KJ, Park KA, Byun HS, Won M, Hong J, Hur GM, Seok JH, Shong M, Sack R, Brazil DP, Hemmings BA, Park J. Cell Signal. 2009; 21:767–777. [PubMed: 19168126]
5. Parcellier A, Tintignac LA, Zhuravleva E, Cron P, Schenk S, Bozulic L, Hemmings BA. Cell Signal. 2009; 21:639–650. [PubMed: 19168129]
6. Piao L, Li Y, Yang KJ, Park KA, Byun HS, Won M, Hong J, Kim JL, Kweon GR, Hur GM, Seok JH, Cho JY, Chun T, Hess D, Sack R, Maira SM, Brazil DP, Hemmings BA, Park J. BMC Cell Biol. 2009; 10:53. [PubMed: 19604401]
7. Zhao H, Martin BM, Bisoffi M, Dunaway-Mariano D. Biochemistry. 2009; 48:5507–5509. [PubMed: 19453107]
8. Cao J, Xu H, Zhao H, Gong W, Dunaway-Mariano D. Biochemistry. 2009; 48(6):1293–1304. [PubMed: 19170545]
9. Rhodes N, Heerding DA, Duckett DR, Eberwein DJ, Knick VB, Lansing TJ, McConnell RT, Gilmer TM, Zhang S, Robell K, Kahana JA, Geske RS, Kleymenova EV, Choudhry AE, Lai Z, Leber JD, Minthorn EA, Strum SL, Wood ER, Huang PS, Copeland RA, Kumar R. Cancer Res. 2008; 68(7): 2366–2374. [PubMed: 18381444]

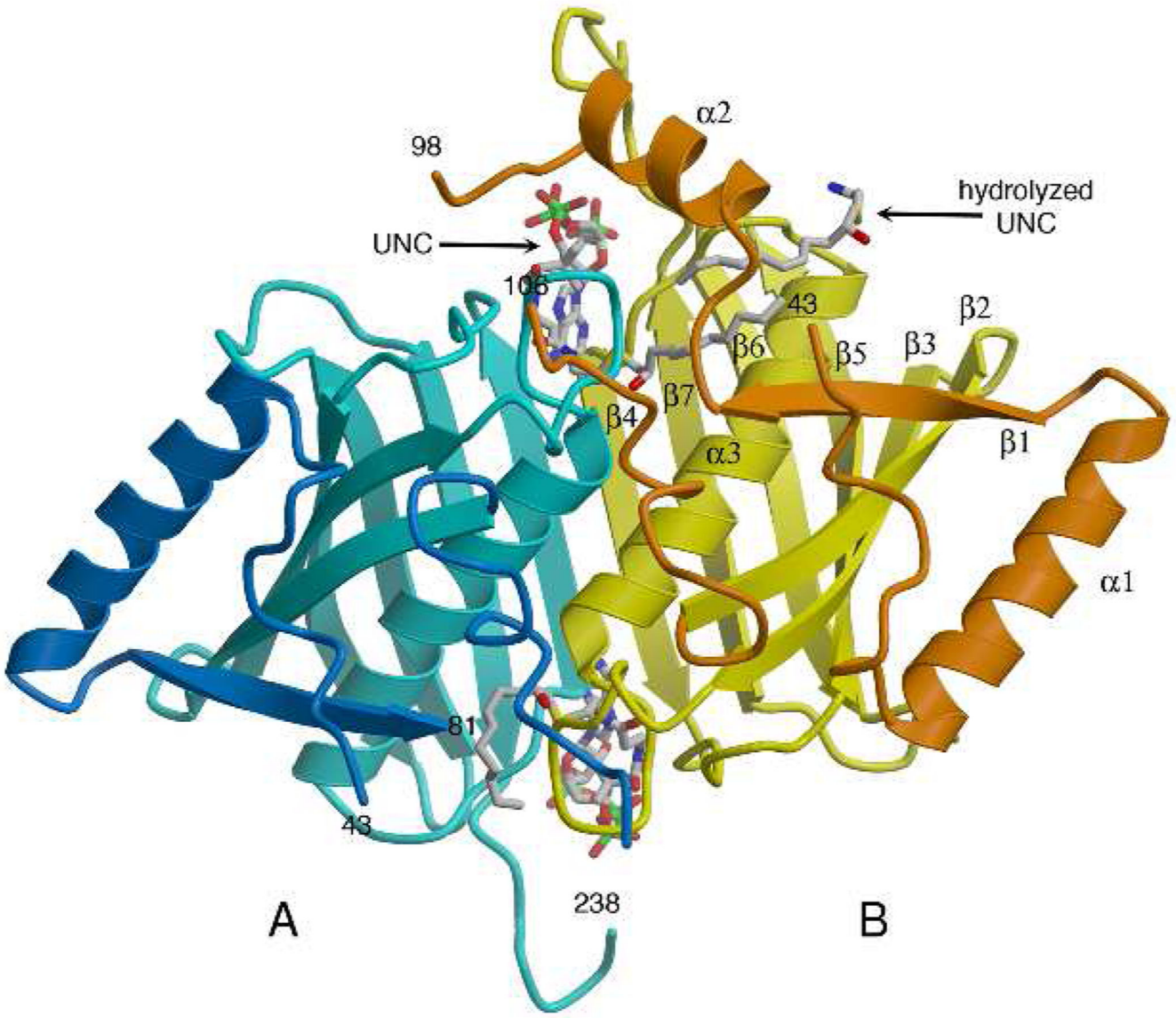

Figure 1.

The hTHEM4 dimer with one molecule of undecan-2-one-CoA (UNC) bound to each subunit (A blue & B yellow; N-domain darker shade) and with a third partially disordered molecule of UNC bound to subunit B (UNC tail).

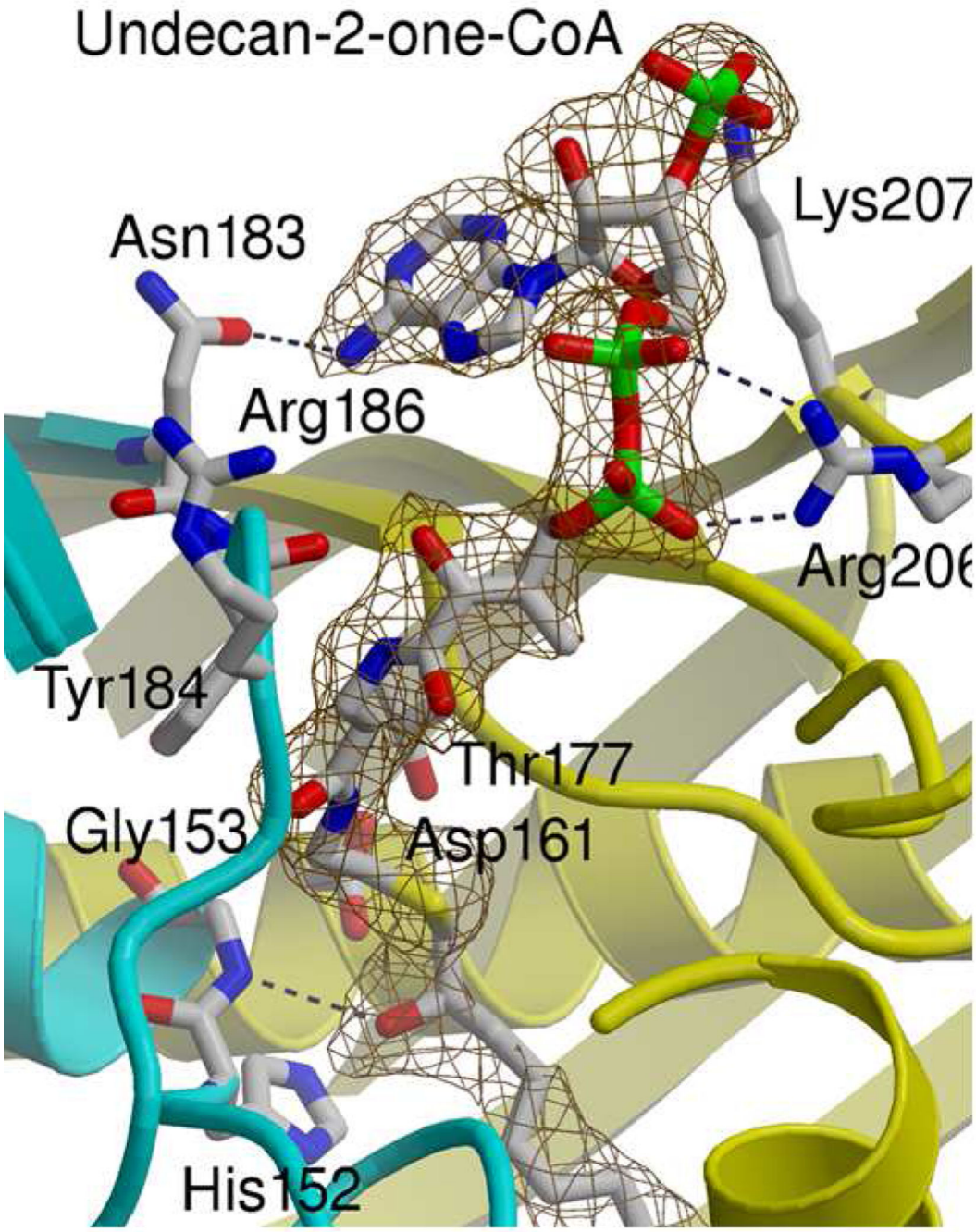

Figure 2.

The hTHEM4 active site bound with undecan-2-one-CoA. The mesh defines the initial difference Fourier electron density with the coefficients Fo-Fc and calculated phases prior to adding the ligand to the model. The map is contoured to 2.5 σ.

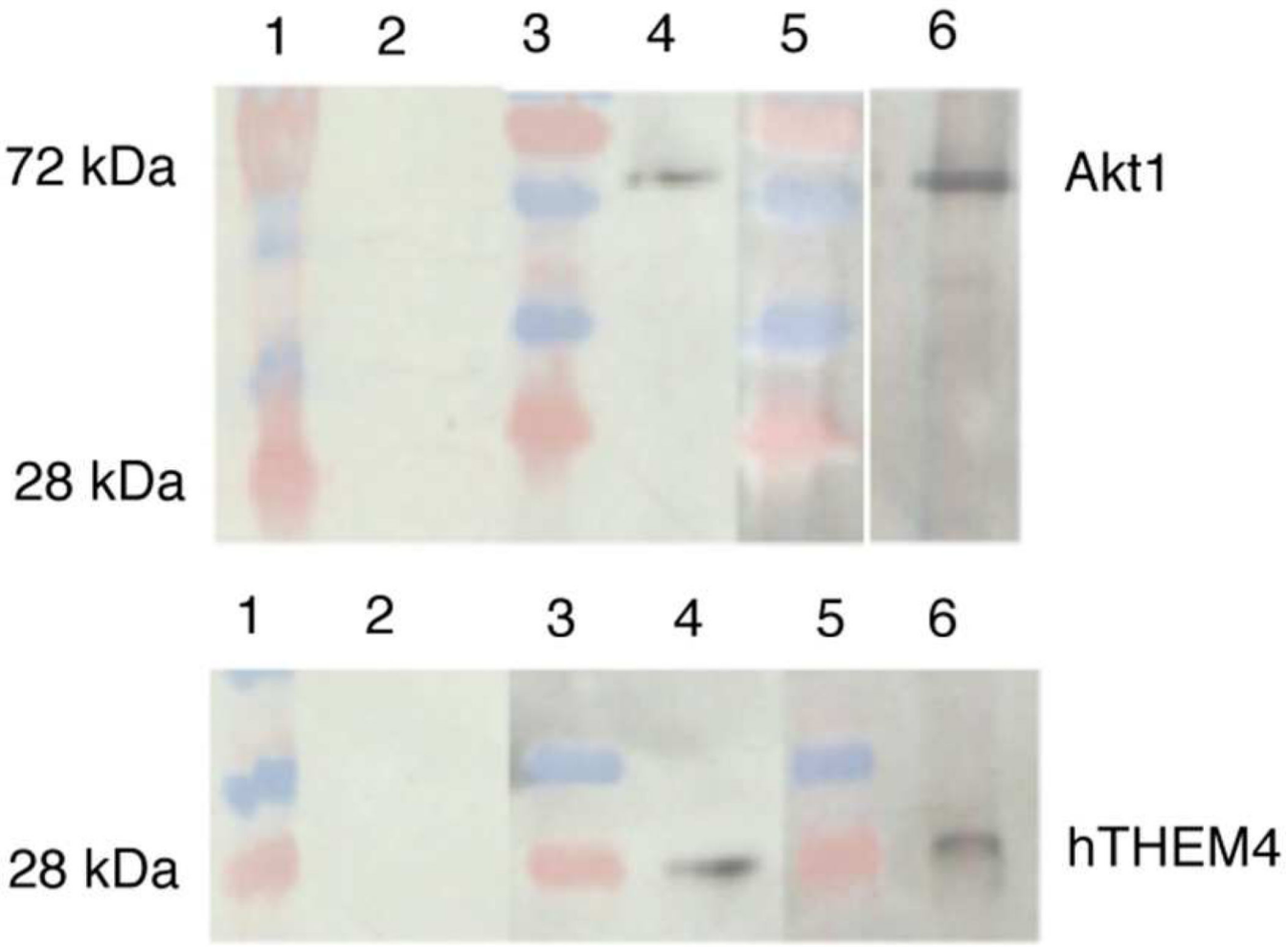

Figure 3.

Western blots of the protein fraction eluted from Akt1 antibody-functionalized agarose beads incubated with 150 μg Akt1 and 35 μg hTHEM4-His_6 Lane 4) or His_6-hTHEM4 (Lane 6). Lane 2 is the protein from the control in which Akt1 was omitted. Lanes 1, 3 and 5 contain Ruler Plus Prestained Ladder. The top immunoblot was developed using anti-Akt1 antibody and the bottom using anti-hHTEM4 antibody.

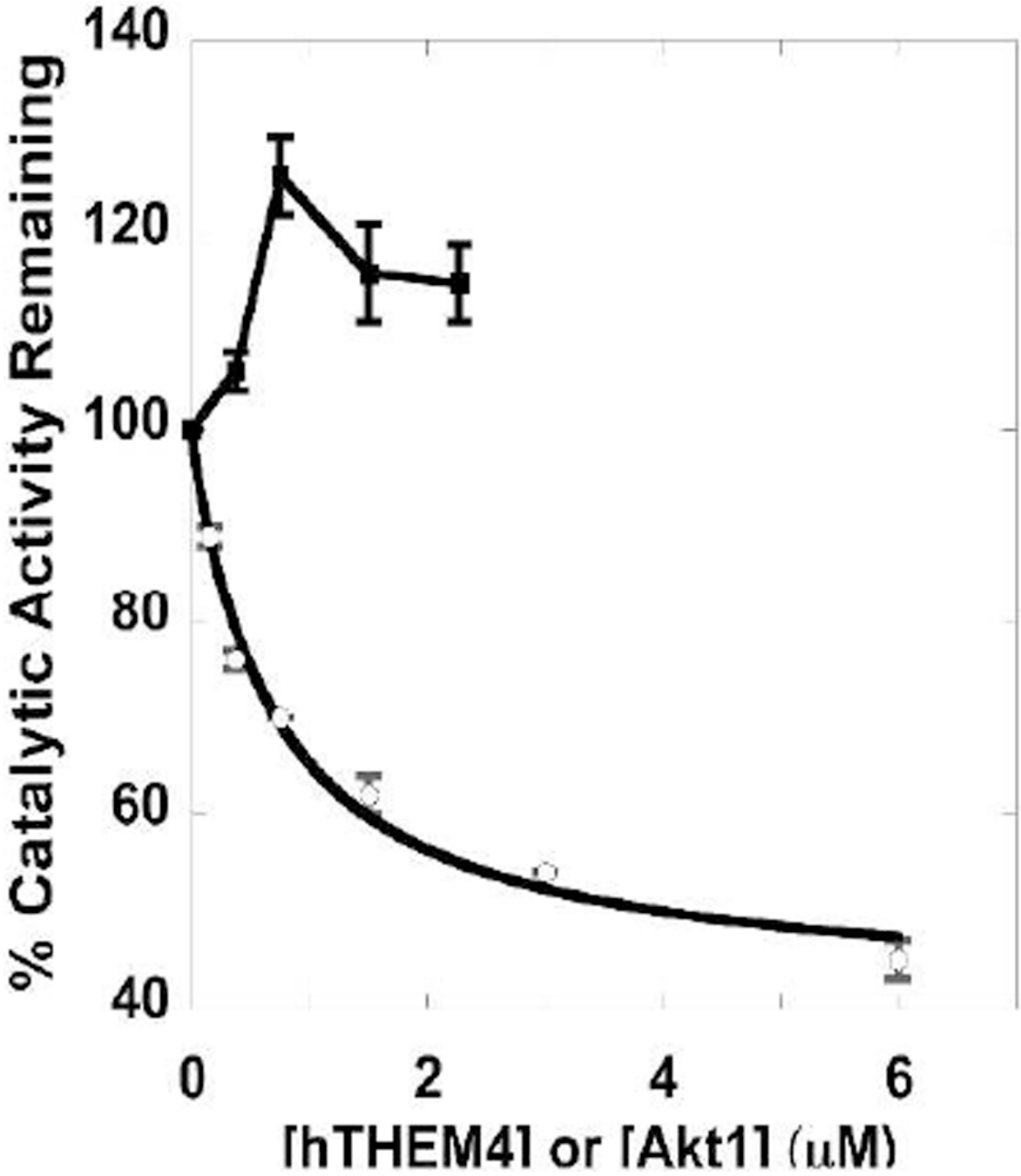

Figure 4.

Plots of the % Akt1 kinase activity *vs* the concentration of hHTEM4 (○) and % hTHEM4 activity *vs* the concentration of Akt1 (■). The error bars represent the standard deviation of triplicate data points. See SI for details.

Table 1

Steady-state kinetic constants of wild-type and mutant hHTEM4-catalyzed hydrolysis of myristoyl-CoA at pH 7.5 and 25 °C. See SI for details.

hTHEM4	k_{cat} (s^{-1})	K_m (μM)	k_{cat}/K_m (M^{-1} $s^{-}1$)
wild-type	4.2 ± 0.1	2.4 ± 0.1	1.7×10^6
D161E	0.1 ± 0.01	45 ± 3	2.3×10^3
D161N	0.07 ± 0.01	300 ± 100	2.0×10^2
T177A	0.07 ± 0.01	4.0 ± 0.1	1.8×10^4
H152F	0.03 ± 0.01	1.1 ± 0.1	2.7×10^4
H152A	0.04 ± 0.01	62 ± 4	6.7×10^2
R206A	1.5 ± 0.1	4.4 ± 0.6	3.6×10^5
K207A	1.5 ± 0.1	2.8 ± 0.1	6.7×10^5
N183A	5.0 ± 0.1	1.6 ± 0.1	1.2×10^2